Desalination and Water Treatment
www.deswater.com

doi:10.5004/dwt.2016.11341

61 (2017) 262–273
January

Performance analysis of power, desalination and cooling poly-generation system using parabolic trough solar collectors

Esa Dube Kerme[a], Jamel Orfi[a,*], Philip Davies[b]

[a]*Department of Mechanical Engineering, College of Engineering King Saud University, Riyadh, Saudi Arabia, email: esadube@gmail.com (E.D. Kerme), orfij@ksu.edu.sa (J. Orfi)*
[b]*Sustainable Environment Research Group, School of Engineering and Applied Science, Aston University, Birmingham, UK email: p.a.davies@aston.ac.uk*

Received 6 February 2016; accepted 13 June 2016

ABSTRACT

This work presents a thermodynamic analysis of a poly-generation system powered by solar energy using parabolic trough solar collectors. The system is composed of an organic Rankine cycle (ORC), a multiple effect distillation and an absorption cooling unit. The analysis is based on the solution of mass, energy and exergy balances of the set of equations of all the components of the system. It is also based on the technical specifications of sub-systems and working fluid properties. The validation of the computer program is achieved systematically. The performance of the poly-generation plant is investigated under Riyadh weather conditions and for several conditions of the operating parameters. The variation of the energy rates required for desalination, cooling and electricity generation has been obtained for two representative days in summer and winter of 2013 in Riyadh. Results expressing the plant performance using the energy and exergy efficiencies are presented and discussed. Specifically, energy utilization factor, artificial thermal efficiency, fuel energy saving factor and exergy efficiency were introduced and used as plant performance indicators. The fresh water production rate and the power to water ratio were also evaluated for two representative days in June and January of 2013. The main results of the study show that although there is a clear dispersion of the obtained values for the performance of the solar poly-generation plant, the exergy efficiency and the fuel energy saving factor give close values.

Keywords: Solar energy; Multi-generation; MED; Organic Rankine cycle; Absorption cooling; Exergy analysis

1. Introduction

Nowadays energy needed for different applications including cooling, power generation, desalination and air conditioning is mainly generated by burning conventional energy sources such as oil and natural gas. These energy sources have a limited life and release harmful gases during operation. Several attempts have been proposed to change energy production, supply and consumption methods in order to reduce the environmental impacts associated with the use of conventional energy sources [1–3]. In other words, an effort has to be made in order to make the recent energy utilization cleaner, more sustainable, efficient and economical. The development of energy efficient technologies such as poly-generation and hybrid systems and the use of renewable energy sources are attractive ways to satisfy the above targets. Poly-generation systems are known to have high overall efficiencies, low operating costs and low pollution emissions [4,8]. On another side, solar energy becomes the most promising

*Corresponding author.

Presented at EuroMed 2015: Desalination for Clean Water and Energy Palermo, Italy, 10–14 May 2015. Organized by the European Desalination Society.

candidate to be directly used as a primary energy source for energy supply systems [5–7].

Poly-generation systems simultaneously produce power, heating, cooling and/or desalination all from the same energy source. A typical poly-generation system comprises energy source, a prime mover, electricity generator, thermally activated technologies (such as absorption chiller and desalination unit) and heat recovery unit.

Many authors have proposed and assessed different configurations of poly-generation systems [9–13]. Serra et al. [9] discussed concepts of poly-generation and energy integration by providing examples in application areas such as a sugar cane factory (for sugar and energy production), district heating and cooling with natural gas cogeneration engines and combined production of water and energy. They concluded that process integration and poly-generation systems are promising tools in fulfilling the double objective of increasing the efficiency of natural resources and minimizing the environmental impacts. In another study, Nixon et al. [10] assessed the feasibility of hybrid solar-biomass power plants to be employed in the poly-generation applications such as electricity generation and process heat. They conducted studies in peak thermal capacities varying from 2 MW to 10 MW using technical, financial and environmental criteria. In a different study, small scale hybrid solar powered heating, chilling and power generation system with parabolic trough collector using cavity receiver, a helical screw expander and silica gel–water adsorption chiller was proposed and extensively investigated by Zhai et al. [11]. Their study indicated that both the main energy and exergy losses take place at the parabolic trough collector. It was also found that the system has higher solar energy conversion efficiency than conventional solar thermal power generation system alone. In addition, Al-Sulaiman et al. [12] carried out energy and exergy analyses of a biomass tri-generation system using an organic Rankine cycle (ORC). Four cases including single electrical power production, power production-cooling, power production-heating and tri-generation were analyzed with respect to pinch point temperature of ORC evaporator, inlet temperature and pressure of the pump. The main exergy destruction was found to occur in the biomass burner (with 55% contribution) and ORC evaporator with 38% contribution. Simultaneous energy and water generation system through the organic Rankine cycle (ORC) prime mover for heat and power generation, multi-effect distillation (MED) water desalination and cooling was assessed by Maraver et al. [13]. They analyzed the energy feasibility of the configuration by using fuel energy saving ratio (FESR). They found that the highest savings correspond to the complete use of heat for domestic hot water which limits the amount of heat used for the activation of MED and thermally activated subsystems. They modeled ORC subsystem using several working fluids for the ORC poly-generation application. They concluded that fluorobenzene and octamethyltrisiloxane could be the most suitable organic fluids for the proposed ORC poly-generation system.

The importance of poly-generation systems with regard to environmental saving and sustainability was investigated by some authors [14,15]. Wang et al. [14] analyzed the performance and emission characteristics of a household sized tri-generation with a diesel engine generator prime mover fuelled with hydrogen. Their results also indicated that large potential fuel savings and reductions in greenhouse gas emissions per unit of useful energy outputs were obtained with tri-generation compared to single generation systems.

The concept of exergy and its relation with environment, sustainability and energy management has been discussed in several works including those of Ugur et al [15], Kanuglu et al. [16] and Dincer and Rosen [17]. Besides, a number of researchers have showed the significance of exergy analysis in assessing power plants with combined heat and power (CHP) and tri-generation systems [18]. Minciuc et al. [19] presented a method for analyzing tri-generation systems and establishing limits for the best performance of gas turbine tri-generation with absorption chilling from a thermodynamic perspective. Ahmadi et al. [20] studied exergo-environmental analysis of an integrated organic Rankine cycle for tri-generation. They obtained that exergy efficiency of the tri-generation system is higher than that of typical combined heat and power systems or gas turbine cycles. Their results also indicate that carbon dioxide emissions for tri-generation system are less than the other combined systems.

The assessment of performance of poly-generation systems is based on various criteria and definitions. The widely used ones consider the energetic efficiency (or the utilization factor) where power and heat, have the same value ignoring their respective quality. Exergy combining the first and second laws of thermodynamics is also used. Therefore, the performance is defined from quantitative as well as qualitative points of view. Minciuc et al. [19] noticed that in a poly-generation system and since the cooling sub-system can use a refrigeration machine with COP higher than 1, the overall system efficiency can be higher than 1 too. The authors presented discussions on several definitions for the performance of poly-generation. The fuel energy saving ratio is employed in several studies as a reliable criteria among the existing thermodynamic performance criteria for cogeneration and poly-generation systems [21–23].

Producing fresh water using a dual or multi-purpose plants is accepted as a reliable and efficient way compared to the single purpose desalination plants. El Nashar [24] reviewed the state of the art of cogeneration for power and desalination. He described a methodology for the selection of optimum configuration for a given water and power demand. Helal [25] and Zak et al. [26] reviewed several configurations of hybrid membrane/distillation desalination and power plants.

The use of solar energy to drive desalination and electric generation plants has gained a significant attention reflected in several studies [27,28]. Palenzuala et al. [29] proposed and assessed different configurations of combined parabolic trough solar collectors and power and desalination plants under arid weather conditions and different steam extractions of the turbine.

The objective of this study is to perform a thermodynamic analysis of a solar driven poly-generation system integrated with ORC as a prime mover. The analysis and the evaluation of the proposed poly-generation system are carried out by studying the variation of energy rates for desalination, cooling and electricity generation for two typical days in summer and winter in 2013 in Riyadh.

The performance of the overall system is also investigated using various performance indicators based on energy and exergy.

2. Description of the system

The system considered in this study encompasses a parabolic trough solar collector (PTSC), a power producing (ORC), multi-effect water distillation (MED) and a single effect absorption cooler (Fig. 1).The system produces electric power, water and cooling simultaneously.

To design an efficient ORC, selection of an appropriate working fluid is crucial. One important criterion for the selection of working fluid is that it should have high critical temperature so that the waste heat can be used more efficiently. Other criteria include the size of equipment, cycle efficiency and environmental impacts [30,31]. O-xylene is selected here as the working fluid due to its relatively high critical temperature (630 K) and the high total efficiency that it provides.

The solar energy collecting system is a field of 'Sky Trough' parabolic trough solar collector modules each of length 14 m [32]. The receiver pipe carrying the heat transfer fluid (Therminol VP-1) has a vacuum annulus to reduce heat losses (see Table 1 for details). Therminol VP-1 has been selected in this study because of its exceptional heat stability and low viscosity for efficient and uniform performance in a wide range of operating temperature of 12–400°C [33]. It has already been used in many different power plants driven by PTC solar collectors [34,35]. Since the solar energy input varies with time over the day, solar driven poly-generation system is a dynamic system. So, in order to have a continuously operating solar powered system, thermal storage system is crucial, and it stores the excess solar energy during the day time so that the system can run during the night time when there is no solar energy. Due to this fact, thermal storage has been integrated into the system under consideration.

3. Analysis of the poly-generation system

The developed model is based on energy and exergy analysis of the multi-generation system. The obtained equations are programmed and solved with the help of

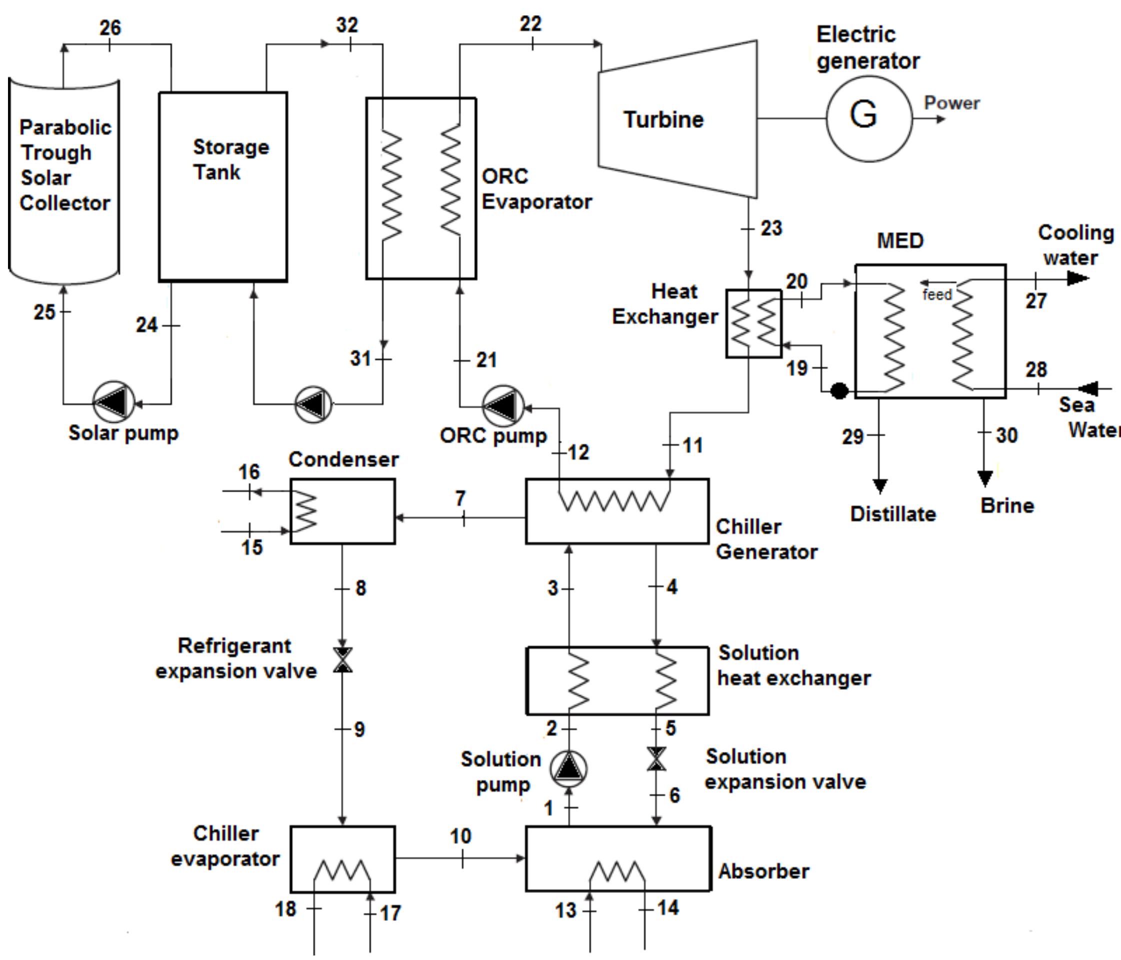

Fig. 1. Schematic of the solar driven poly-generation system for electric power generation, desalination and cooling.

engineering equation solver software (EES) [36]. To simplify the theoretical analysis of the system under consideration, the following assumptions are considered:

- The system runs at quasi- steady state throughout.
- Pressure drops and heat losses in pipelines as well as in heat exchangers are neglected.
- The working fluid at the pump inlet of ORC is saturated liquid.
- The refrigerant at the outlet of the condenser and evaporator of the absorption chiller system are saturated liquid and saturated vapor respectively.
- Work input by the pump of the absorption chiller system is neglected, as it is very small as compared to the heat input to the generator.
- Kinetic and potential energies as well as their exergies are ignored.
- Chemical exergy of materials (except for the salty water analysis in the MED system) is neglected.
- The steam supplied to MED is assumed to be saturated steam.
- Feed water temperature and cooling water temperature in MED system are calculated in such a way that their difference is 10°C.
- The bottom brine boiling temperature and feed water temperature in the MED system are chosen such that their difference is 5°C.
- Dead state properties for all fluids are evaluated at: T_o = 25°C and P_o = 101.325 kPa and the dead state salinity (for Arabian Gulf seawater), X_o= 42g kg^{-1}

3.1. Energy analysis

3.1.1. Solar energy collecting system

Modeling of the solar parabolic trough collector (PTC) subsystem is based on the equations presented in [35,37–38]. The rate of useful energy delivered from a PTC is defined as:

$$Q_u = A_{ap}F_R(S - \frac{A_r}{A_{ap}}U_L(T_{fi} - T_a)) \tag{1}$$

where F_R is the heat removal factor, S is the heat absorbed by the receiver, A_{ap} is the aperture area, A_r is the receiver area, and U_L is the solar collector overall heat loss coefficient. The heat absorbed by the receiver is defined as:

$$S = G_b\eta_r \tag{2}$$

Table 1a
Input data used in the ORC sub-system analysis

Parameters	Value
Isentropic turbine efficiency, %	85
Isentropic pump efficiency, %	85
Motor efficiency, %	95
Generator efficiency, %	95
Turbine inlet pressure, MPa	2
Pump inlet temperature, °C	95

Table 1b
Input data used in the PTC sub-system analysis

Parameters	Value
Aperture width, m	6
PTC Length per module, m	14
Receiver Inner diameter, m	0.08
Receiver Outer diameter, m	0.0889
Glass cover diameter, m	0.125
Transmissivity of the receiver	0.94
Absorptivity of the receiver	0.97
Reflectivity of the aperture surface	0.96
Intercept angle	1
Receiver emittance	0.92
Glass cover emittance	0.87
Mass flow rate of heat transfer fluid, kg s^{-1}	4.5
Overall heat conductance of storage tank, kW K^{-1}	0.111

Table 1c
Input data used in the absorption chiller sub-system analysis

Parameters	Value
Solution heat exchanger effectiveness	0.64
Solution pump mass flow rate, kg s	2
Cooling water mass flow rate to absorber, kg s^{-1}	13.42
Cooling water inlet temperature, °C	25
Cooling water mass flow rate to condenser, kg s^{-1}	10.72
Chilled water mass flow rate, kg s^{-1}	25.26
Chilled water inlet temperature, °C	14
Overall heat conductance of generator, kW K^{-1}	1.4
Overall heat conductance of condenser, kW K^{-1}	1.8
Overall heat conductance of evaporator, kW K^{-1}	2
Overall heat conductance of absorber, kW K^{-1}	2.1

Table 1d
Input data used in the MED sub-system analysis

Parameter	Value
Steam delivery temperature, °C	90
Cooling water temperature, °C	25
Salinity of the brine, g kg^{-1}	70
Salinity of cooling water, g kg^{-1}	42
Number of effects	10

where G_b is the direct irradiation intensity and η_r is receiver efficiency which is defined as

$$\eta_r = \rho\gamma\tau\alpha K \tag{3}$$

where ρ, γ, τ, α and K are the reflectance of the mirror, intercept factor, transmittance of the glass cover, absorptance of the receiver and incidence angle modifier respectively. The heat removal factor is given by:

$$F_R = \frac{m_r C_{pr}}{A_r U_L}\left[1 - \exp\left(-\frac{A_r U_L F_l}{m_r C_{pr}}\right)\right] \tag{4}$$

where m_r is mass flow rate through the receiver, C_{pr} is the specific heat of heat transfer fluid inside the receiver and F_l is the collector efficiency factor defined as:

$$F_l = \frac{1/U_L}{\frac{1}{U_L} + \frac{D_o}{D_i\,h_{fi}} + \frac{D_o}{2k}\ln\left(\frac{D_o}{D_i}\right)} \tag{5}$$

where k is the thermal conductivity of the receiver tube and h_{fi} is the convection heat transfer coefficient inside the receiver tube and it can be obtained from:

$$h_{fi} = \left(\frac{Nu\,k_{fi}}{D_i}\right) \tag{6}$$

where Nu is the Nusselt number which can be obtained from the standard pipe flow equation [37]:

$$Nu = 0.023\,\mathrm{Re}^{0.8}\,\mathrm{Pr}^{0.4} \tag{7}$$

where Re is the Reynolds number and Pr is the Prandtl number of the flow inside the receiver tube.

The solar collector heat loss coefficient between ambient and receiver is defined as:

$$U_L = \left[\frac{A_r}{(h_{c,ca} + h_{r,ca})A_c} + \frac{1}{h_{r,cr}}\right]^{-1} \tag{8}$$

The radiation heat coefficient between the ambient and the cover is given by:

$$h_{r,ca} = \varepsilon_c\sigma\left(T_c + T_a\right)\left(T_c^2 + T_a^2\right) \tag{9}$$

where σ is Stefan–Boltzmann constant and ε_c is the emittance of the cover. The radiation heat transfer coefficient between the cover and the receiver is defined as:

$$h_{r,cr} = \sigma\frac{\left(T_c + T_r\right)\left(T_c^2 + T_r^2\right)}{1/\varepsilon_r + (A_r/A_c)\left(1/\varepsilon_c - 1\right)} \tag{10}$$

where T_r is the receiver average temperature. The convection heat loss coefficient between the ambient and the cover is defined as:

$$h_{c,ca} = \left(\frac{Nu\,k_{air}}{D_{co}}\right) \tag{11}$$

where k_{air} is the thermal conductivity of the air. The cover temperature of the receiver is obtained by the equation:

$$T_c = \frac{A_r h_{r,cr} T_r + A_c\left(h_{c,ca} + h_{r,ca}\right)T_a}{A_r h_{r,cr} + A_c(h_{c,ca} + h_{r,ca})} \tag{12}$$

The total amount of solar radiation that shines up on collector field, which is the total energy input to the system is defined as:

$$\dot{Q}_{solar} = A_{ap}\,F_R\,S\,N_t \tag{13}$$

where N_t is the total number of collectors and A_{ap} is the aperture area which is obtained as:

$$A_{ap} = (w - D_{co})L \tag{14}$$

where L, w, and D_{co} are the collector (module) length, width and receiver cover outer diameter respectively.

In this study, sensible thermal storage system is integrated with the system under consideration to store the collected solar energy and provide continuous heat supply. To simplify the model, it is assumed that the liquid (Therminol VP-1) in the insulated storage tank is completely mixed with the liquid (Therminol VP-1) flowing back into the tank from the collector and ORC evaporator as shown in Fig. 1. By making an energy balance on the un-stratified (i.e. fully mixed) tank, the following equation can be obtained [38]:

$$\left[(mC_p)_s\right]\frac{dT_s}{dt} = Q_u - Q_{load} - (UA)_s.(T_s - T_a) \tag{15}$$

where m is the mass of fluid (Therminol VP-1) in the storage unit and C_p is the specific heat capacity of fluid (Therminol VP-1) in the storage. T_a is the ambient temperature around the tank. Q_u and Q_{load} represent the useful gain from the solar collector and the energy needed by the absorption system respectively. $(UA)_s$ is the liquid storage tank loss coefficient-area product. If Q_u and Q_{load} and tank losses over the time period of Δt are assumed to be constant, Eq. (15) can be written for each time interval as [38]:

$$T_s^+ = T_s + \frac{\Delta t}{mC_p}\left[Q_u - Q_{load} - (UA)_s.(T_s - T_a)\right] \tag{16}$$

where T_s^+ is the storage tank fluid temperature at the end of time interval Δt .

3.1.2. Organic Rankine cycle system

The organic Rankine cycle subsystem is modeled based on mass and energy conservation laws. In the evaporator, the heat addition into the power cycle is given by:

$$\dot{Q}_E = \dot{m}_f(h_{22} - h_{21}) \tag{17}$$

where $\dot{m}_f$ is the mass flow rate of the organic working fluid. For the turbine, the isentropic efficiency is expressed as:

$$\eta_T = \frac{h_{22} - h_{23}}{h_{22} - h_{23s}} \tag{18}$$

The power output of the turbine is given by:

$$\dot{W}_T = \dot{m}_f (h_{22} - h_{23}) \tag{19}$$

For the pump, the isentropic efficiency can be expressed as:

$$\eta_p = \frac{h_{21s} - h_{12}}{h_{21} - h_{12}} \tag{20}$$

The ORC pump power consumption is defined as:

$$\dot{W}p_{,ORC} = \dot{m}_f (h_{21} - h_{12}) \tag{21}$$

The power input to the solar pump is given by:

$$\dot{W}p_{,solar} = \dot{m}_t (h_{25} - h_{24}) \tag{22}$$

where $\dot{m}_t$ is mass flow rate of heat transfer working fluid (Therminol VP-1). The net electrical power output generated by the system is given by:

$$\dot{W}_{net,el} = \dot{W}_T \eta_g - \dot{W}_{p,ORC} / \eta_{motor} - \dot{W}_{p,solar} / \eta_{motor} \tag{23}$$

where η_g and η_{motor} are generator and motor efficiencies respectively.

3.1.3. Absorption chiller system

In the absorption chiller system, a mixture of LiBr and H_2O has been used as a working fluid. The LiBr-H_2O absorption cooling subsystem is modeled based on the laws of mass and energy conservations by taking control volume across each of the components: generator, condenser, evaporator, heat exchanger and absorber. The rate of heat supplied to the generator, which is the rate of energy input to the chiller cycle, is obtained from the heat balance as in the following equation:

$$Q_{gen} = m_7 h_7 + m_4 h_4 - m_3 h_3 \tag{24}$$

The rate of heat rejection out of the condenser is given by the following equation:

$$Q_{cond} = m_7 h_7 - m_8 h_8 \tag{25}$$

The rate of heat removal from the absorber is:

$$Q_{abs} = m_{10} h_{10} + m_6 h_6 - m_1 h_1 \tag{26}$$

The rate of heat added to the evaporator is the cooling effect produced by the absorption cooling system, as follows:

$$Q_{chiller,evap} = m_{10} h_{10} - m_9 h_9 \tag{27}$$

The energy balance on the hot side of the solution heat exchanger is given by the following equation:

$$Q_{hx-h} = m_4 h_4 - m_5 h_5 \tag{28}$$

Similarly the energy balance on cold side of the solution heat exchanger is given by the following equation:

$$Q_{hx-c} = m_3 h_3 - m_2 h_2 \tag{29}$$

The energy balance on the solution heat exchanger is satisfied if $Q_{hx-h} = Q_{hx-c}$.

Defining X as Lithium bromide concentration, which is the ratio of the weight of Lithium Bromide to the weight of LiBr-H2O solution, a concentration balance for the generator gives

$$X_3 m_3 = X_4 m_4 \tag{30}$$

3.1.4. MED desalination system

The amount of energy needed to supply the saturated steam required by the MED system is given by:

$$\dot{Q}_{MED} = m_{19}(h_{20} - h_{19}) \tag{31}$$

The overall mass balance around the MED plant assuming that the product (distillate water) is free of salt ($x_d = 0$) gives:

$$m_f = m_b + m_d \tag{32}$$

$$m_f x_f = m_b x_b \tag{33}$$

where m is the mass flow rate, x is the salinity, and the subscripts b, d, and f denote the rejected brine, distillate, and feed seawater respectively. The thermal performance PR of the MED plant is defined as the mass of distillate water produced per unit mass of heating steam used. That is

$$PR = \frac{m_d}{m_s} \tag{34}$$

where m_d is the total mass of the distillate produced in all effects of MED plant. The specific cooling water flow rate, sM_{cw}, is defined by:

$$sM_{cw} = \frac{m_{cw}}{m_d} \tag{35}$$

To facilitate the analysis of MED system, the following design correlations developed by El-Dessouky et.al [39] for PR and sM_{cw} have been used:

$$\begin{aligned} PR = {} & 1.33 + 7.5510^{-1} n_e - 7.5210^{-3} n_e^2 \\ & + 2.05710^{-2} T_s - 1.4810^{-4} T_s^2 - 3.0810^{-4} n_e T_s \end{aligned} \tag{36}$$

$$sM_{cw} = 35.064 - 5.808 n_e + 2.1910^{-1} n_e^{\,2} + 2.210^{-2} T_s - 10^{-3} T_s^{\,2} + 910^{-3} n_e T_s \tag{37}$$

where n_e is the number of effects in MED and T_s is the temperature of heating steam supplied to MED unit. The vapor temperature T_v in each effect of MED system is defined in terms of the brine boiling temperature (T_b) at each effect and the boiling point elevation (BPE) as [39]:

$$T_b = T_v + BPE \tag{38}$$

The present model of the MED unit is based on design correlations relating the unit thermal performance, specific heat transfer area and specific cooling water mass flow rate to the top brine temperature and the number of effects. Such correlations were developed in a systematic and exhaustive analysis of a forward feed MED plant [39]. The accuracy of the model of [39] had been recently confirmed in the work of Mistry et al. [40]. On the other side, the number of effects taken in our study is 10. This number is commonly used in the actual MED desalination plants and also in the available previous studies in this field. Kamali et al. [41] and Zhao et al. [42] investigated the effect of the number of effects n on the gain output ratio (GOR). In both studies, it was found that this effect is significant for low n. For higher n (between 8–10), the increase in GOR is not as important as for lower n. This explains the use of this specific value of 10 of the effects number. It is also important to say that using a close number such as 8 or 9 should lead qualitatively to the same kind of results.

The thermo-physical properties of sea water at each point around the MED desalination system are calculated by using sea water library developed inside EES software [36].

3.2. Exergy analysis

Exergy analysis permits many of the shortcomings of energy analysis to overcome and is useful in identifying the causes, locations, and magnitudes of the process inefficiencies. The exergy destruction is an important parameter in exergy analysis. It is defined as the potential work lost due to irreversibility. The total exergy destruction of the solar driven system considered in this study is the sum of the exergy loss in each component. The exergy destruction rate of a control volume at steady state for each component of the system is defined as:

$$\dot{E}_{xd} = \sum_{in} \dot{m}\psi - \sum_{out} \dot{m}\psi + \sum \left(1 - \frac{T_o}{T_k}\right)\dot{Q}_k - \dot{W} \tag{39}$$

where $\dot{E}_{xd}$, ψ and T are the exergy destruction rate, exergy flow and temperature respectively. The subscript o is the value of the property at the surrounding and the subscript k is the property value at state k. The first term on the right-hand side is the sum of the exergy input. The second is the sum of the exergy output, while the third term is the exergy of heat Q, which is transferred at constant temperature T. The last term is the mechanical work transfer to or from the system. Neglecting kinetic and potential exergy, the physical flow exergy per unit mass for a pure substance is defined as [43]:

$$\psi = (h - h_o) - T_o(s - s_o) \tag{40}$$

where h and s are the enthalpy and entropy per unit mass respectively while the terms h_o and the s_o are the enthalpy and entropy values of the fluid at the environmental temperature. In the absorption chiller system, where a binary mixture solution of LiBr and water is used, the concentration of the mixture must be taken into account for exergy calculation. For this reason the exergy of the solution is calculated by [44]:

$$\psi = [h(T,X) - h_o] - T_o[s(T,X) - s_o] \tag{41}$$

where X is the mass fraction of LiBr in the solution of LiBr-H_2O.

Exergy at each point of the MED system is calculated by using the seawater library developed inside EES software.

The overall exergy input to the solar powered system under consideration is the exergy of the solar radiation falling on the solar collector, and it is the function of the sun's outer surface temperature (T_s = 6000 K) and defined as [35]:

$$\dot{E}x_{,in} = A_c G_b \left(1 + \frac{1}{3}\left(\frac{T_{amb}}{T_s}\right)^4 - \frac{4}{3}\left(\frac{T_{amb}}{T_s}\right)\right) \tag{42}$$

3.3. System performance analysis

This section presents the equations used for the energetic and exergetic performance analysis of cogeneration and poly-generation system shown in Fig.1. In order to quantify the benefits obtained by using multi-generation plants such as tri-generation and poly-generation plants over traditional ones, several evaluation criteria have been formulated. Among these, well-known parameters such as the energy utilization factor (EUF), the primary energy savings (PES), the artificial thermal efficiency (ATE), the fuel energy saving ratio (FESR) and the exergy efficiency (ExE_{ff}) have been developed. Each of these performance indicators considers a particular aspect of energy flows; moreover, they might lead to different conclusions. The energy utilization factor and the artificial thermal efficiency are based on the first law of thermodynamics to see how well energy is used or converted. They give quantitative measures of energy flows without considering their respective quality. The energy utilization factor assesses the overall fuel production efficiency. The artificial thermal efficiency can be used if the electricity production is considered having more weight than the heat production. The fuel energy saving ratio is also a first law indicator. It represents the thermodynamic advantages of multi-generation plants compared to single purpose plants. The exergy efficiency is interesting to compare the poly-generation system against an ideal system based on second law of thermodynamics. Table 2 gives the expression of these performance criteria for the overall poly-generation system.

Table 2
Poly-generation system performance criteria

System	Definition
EUF: Energy utilization factor	$EUF = \dfrac{\dot{W}_{net,el} + \dot{Q}_{evap} + \dot{Q}_{MED}}{\dot{Q}_{solar}}$
ATE: Artificial thermal efficiency	$ATE = \dfrac{\dot{W}_{net,el}}{\dot{Q}_{solar} - (\dot{Q}_{Evap} + Q_{MED}) / \eta_b}$
FESR: Fuel energy saving factor = $\dfrac{\dot{Q}_{Solar-Separate} - \dot{Q}_{Solar-Poly}}{\dot{Q}_{Solar-Separate}}$	$FESR = 1 - \dfrac{\dot{Q}_{Solar-Poly}}{(\dot{W}_{net,el} / \eta_{el}) + (\dot{Q}_{Evap} + Q_{MED}) / \eta_b}$
ExE_{ff}: Exergy efficiency	$\eta_{ex,poly} = \dfrac{\dot{W}_{net,el} + m_{17}(\psi_{18} - \psi_{17}) + m_{19}(\psi_{20} - \psi_{19})}{\dot{E}x_{in}}$

3.4. Model validation

3.4.1. Validation of PTC solar collector model

The solar collector model is validated against the experimental work done by Kutscher et al. [45] as shown in Fig. 2. The collector efficiency variation with temperature difference (between heat transfer fluid temperature and ambient temperature) has been obtained for direct normal solar radiation of 1000W m^{-2}. Fig. 2 indicates that there is an agreement between the present model and the experimental work. However, the collector efficiency of the present work does not accurately fit with experimental collector efficiency data.

3.4.2. Validation of ORC model

The validation of the ORC model is shown in Fig. 3. The figure indicates the thermal efficiency of an ideal Rankine cycle, using R-123 (HCFC-123) as working fluid, calculated by the present model and the results obtained by Hettiarachchi et al. [46]. It can be seen that there is a good agreement between the present results and those of Hettiarachchi et al. [46] for the entire range of turbine inlet temperature.

3.4.3. Validation of absorption cooling system model

The present analysis of the single-effect absorption cooler is validated with Balghouthi et al. [47], who assessed the feasibility of solar-powered absorption cooling technology under the weather conditions of Tunisia. They had modelled the single effect LiBr-H_2O absorption cooling system using the TRNSYS software. They optimized the absorption system with the capacity of 11 kW for a typical building of 150 m^2 total room area. The results of this study show that absorption solar air-conditioning systems are suitable under Tunisian weather conditions. Fig. 4 indicates the coefficient of performance and cooling load versus generator inlet temperature. The figure shows that there is an agreement between the current model of single effect absorption chiller and that of Balghouthi et al. [47].

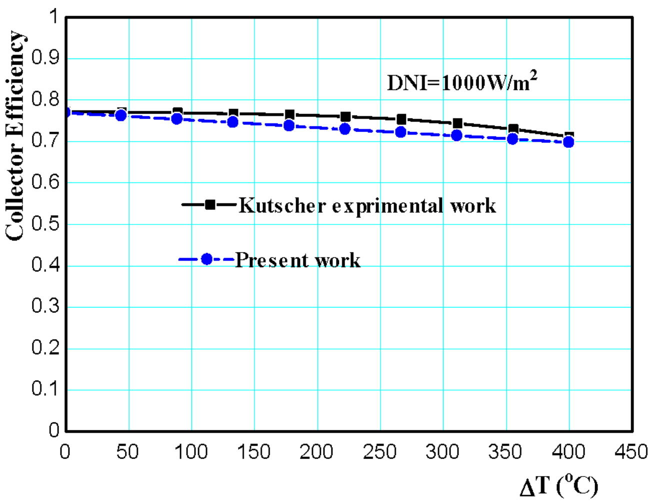

Fig. 2. Validation of the solar collector model: collector efficiency versus temperature difference (DT) between temperature of fluid inside the absorber and ambient.

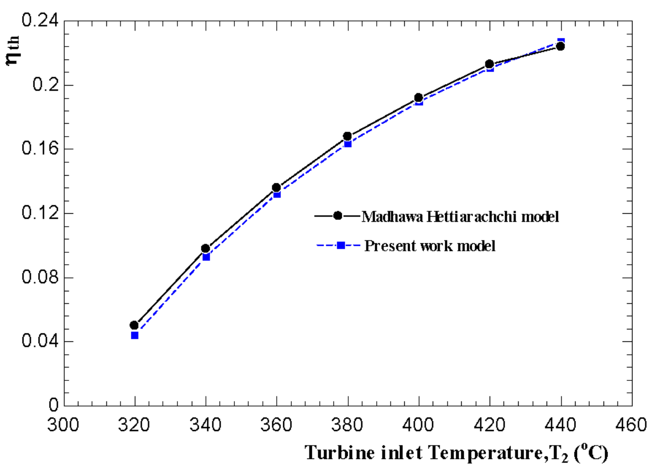

Fig. 3. Validation of the ORC present model with Hettiarachchi et al. [46]: Thermal efficiency versus turbine inlet temperature for an ideal Rankine cycle.

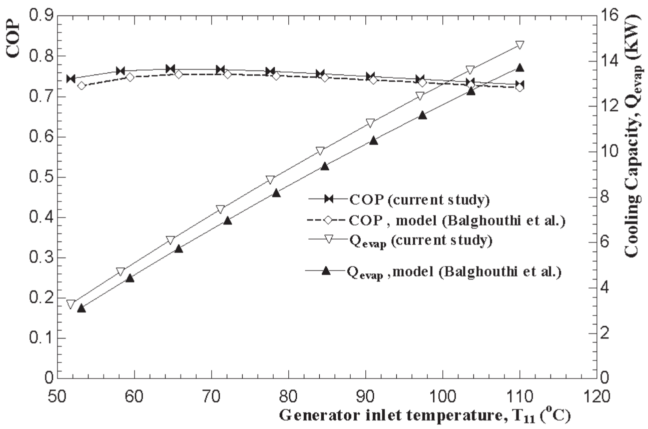

Fig. 4. Validation of the single-effect absorption cooler model as compared to Balghouthi et al.[47] model: COP and cooling capacity versus generator inlet temperature.

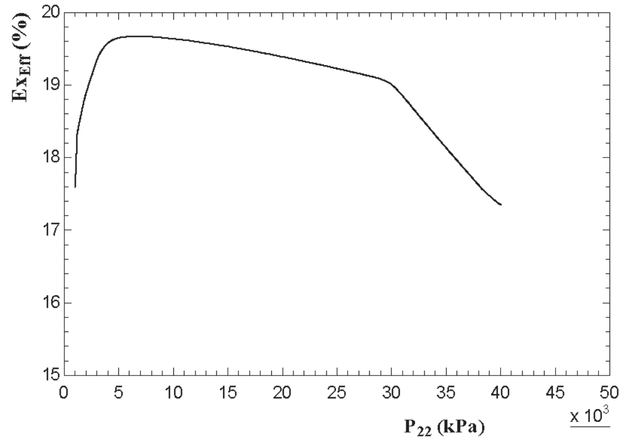

Fig. 5. Total exergy efficienyc variation with turbine inlet pressure P22.

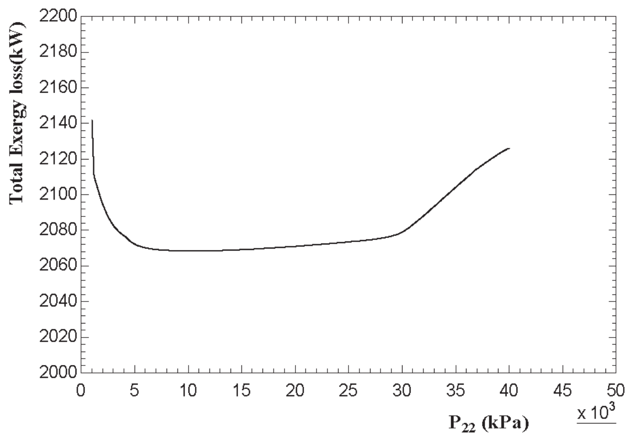

Fig. 6. Total exergy loss variation with turbine inlet pressure P22.

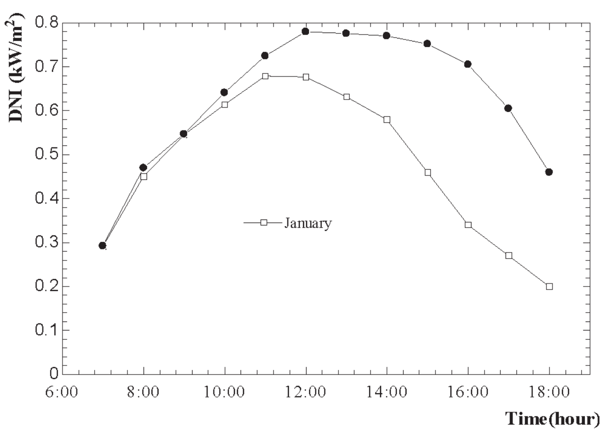

Fig. 7. Direct normal irradiance variation over a day of June and January 21st of 2013 in Riyadh.

4. Results and discussion

This section provides the results of the energetic and exergetic analysis of the solar driven poly-generation system. The conducted energy analysis comprises evaluation of net power output of the system, cooling capacity, heat required to produce saturated steam needed by MED as well as the determination of different performance parameters of the system. In this respect, the trends of different energy rates produced by the solar powered poly-generation system as well as the daily variation of performance evaluation parameters are discussed.

It is worthy to mention that the results were obtained after performing a systematic exergy analysis in which the exergy efficiency is maximum (or total exergy loss of the system is minimum). For instance, The turbine inlet pressure value is calculated based on systematic examination of systems exergetic performance by optimizing the exergetic performance of the system. Based on this fact, the optimization result provides the turbine inlet pressure of 7 MPa which gives the system maximum exergetic efficiency of 19.7% and minimum system total exergy loss of 2068 kW as shown in Figs. 5, 6 respectively. Hence the turbine inlet value has been decided for the analysis based on this fact.

It is known that the area between latitudes 40°N and 40°S is called sun-belt and Saudi Arabia, with latitudes between 31°N and 17.5°N, is conveniently located in the sun-belt, and hence has an abundant available solar energy resources. As a result, in the present work, Riyadh city with (latitude: 24.72°N, longitude: 46.71°E) is selected as the place where the solar driven poly-generation system is built in the simulation work. The direct normal solar radiation intensity (DNI) and ambient temperature variation over the specific day of winter and summer, shown in Figs. 7 and 8 respectively, are used as the basic input parameters for the system simulation. It is easy to understand from Fig. 7 that the solar radiation is the strongest at the midday and is reduced for the rest of the time.

Figs. 9 and 10 illustrate the variation of the system net electric power output, cooling effect and heat required to produce the saturated steam needed by the MED desalination system over the course of the representative day of the year in winter and summer monthes respectively. It can be seen from the figures that the rate of each produced energy starts increasing from the time of sunrise till it reaches its respective peak values at (11: 00 for the day in January and 12:00 for the day in June) and then declines. The figures

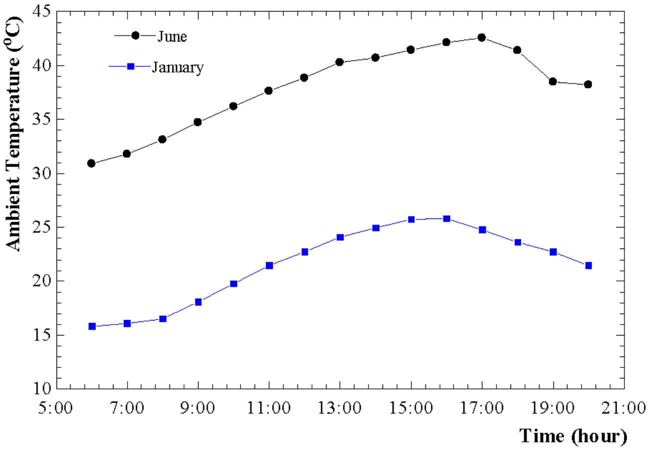

Fig. 8. Variation of ambient temperature over a day of June and January 21st of 2013 in Riyadh.

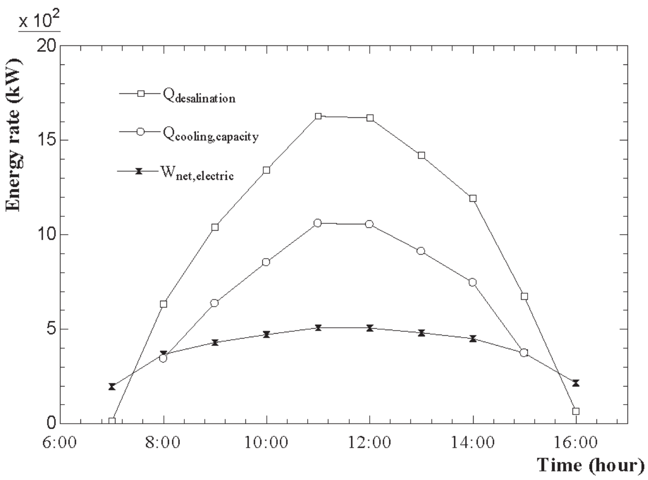

Fig. 9. Variation of energy rates over a day of January 21st of 2013 in Riyadh.

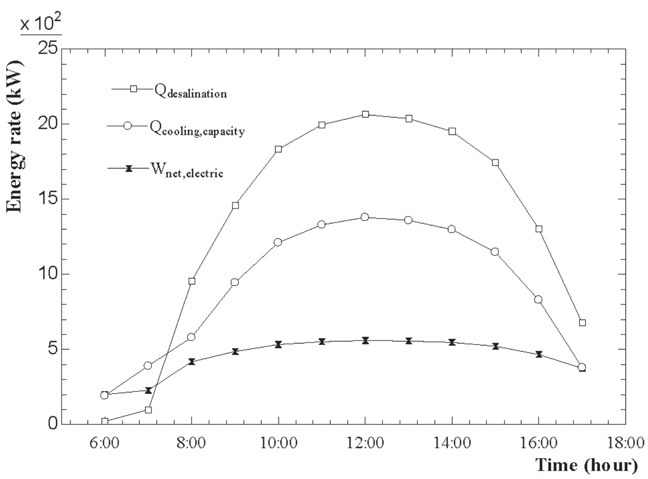

Fig. 10. Variation of energy rates over a day of June 21st of 2013 in Riyadh.

also shows that the trend of the system net power output is somewhat leveled out and quite smooth. The maximum instantaneous power output, cooling capacity and heat of desalination for the winter representative day (January 21st) are 506, 1061 and 1628 kW respectively whereas in the summer month (June 21st) their values are 558, 1350 and 2063 kW respectively. Evidently, the values are greater for the day in the summer month and the operational time of the summer is also greater as compared to the representative day in the month of the winter.

In this work and in order to investigate the performance of the multi-generation system, the four parameters (EUF, ATE, FESR and ExE_{ff}) as defined in Table 3 are considered in Figs. 11 and 12. The figures indicate that all the performance evaluation parameters except exergy efficiency, have the trend similar to the direct normal irradiation intensity presented in Fig. 7. As illustrated in Figs. 11 and 12, the EUF, ATE and FESR vary greatly with time over the day, reaching their respective peak values in the midday around 12:00 and then drop for the rest of the time. Contrary to the other system performance evaluation parameters, the exergy efficiency variation has different

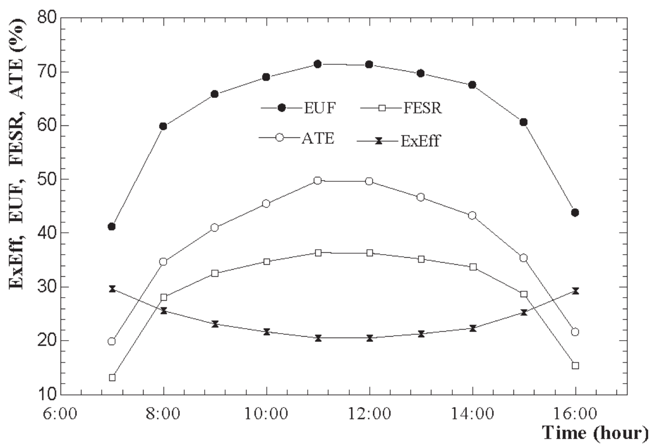

Fig. 11. Variation of performance evaluation of poly-generation system over a day of January 21st of 2013 in Riyadh.

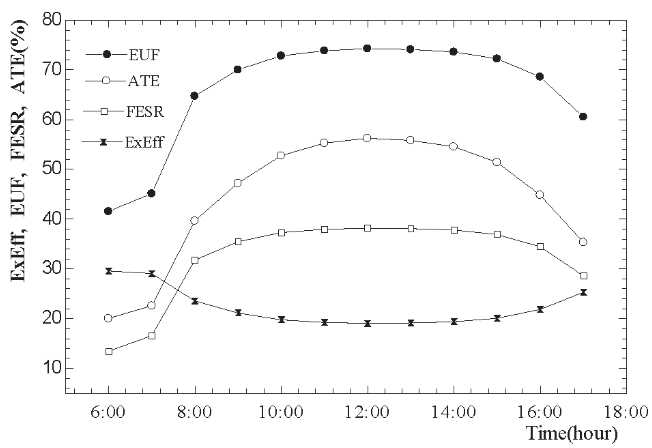

Fig. 12. Variation of performance evaluation of poly-generation system over a day of June 21st of 2013 in Riyadh.

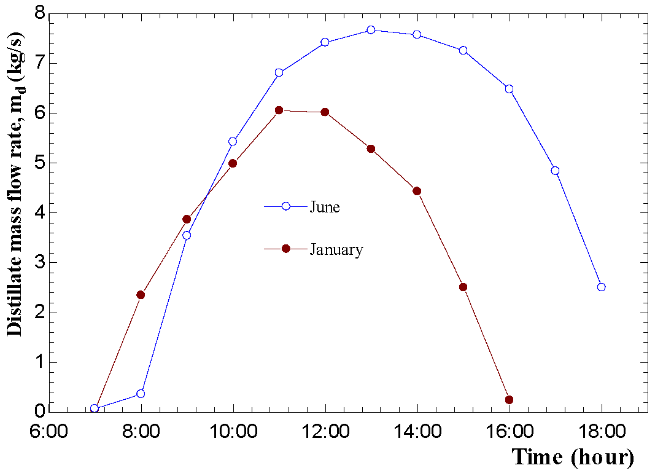

Fig. 13. Evolution of the distillate mass flow rate over a day of June 21st of 2013 in Riyadh.

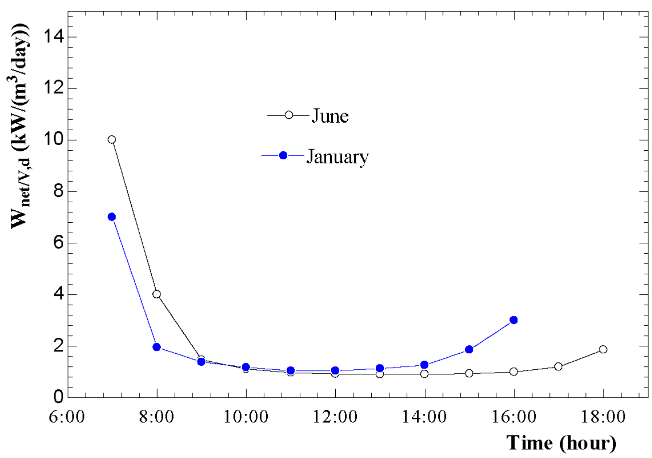

Fig. 14. Evolution of the power to water ratio over a day of June 21st of 2013 in Riyadh.

pattern from that of the other parameters. It has the lowest value during the midday and highest values during the sunrise and sun sets. This is due to the fact that during the midday the exergy destroyed by the system is highest because of high irreversibility associated with high temperature difference between dead state and the system under consideration and vice versa. Comparison between the four different system performance evaluation parameters is also indicated in Figs. 11, 12. The figures present that followed by the artificial thermal efficiency (ATE), the EUF has the highest value than the other system performance evaluation parameters. The Figs. 11 and 12 also illustrate that the system performance evaluation parameters over the day in the summer month (June) have higher values as compared to their respective ones over the representative day in the winter month (January).

On the other side, Figs. 13, 14 give respectively the evolution of the produced fresh water mass flow rate and the power to water ratio over two typical days in June and January of 2013 in Riyadh. The hourly fresh water production can reach 6 kg s^{-1} and 7.6 kg s^{-1} in January and June respectively. Such water production rates can be obtained at about 11:30 AM in January and 1:30 PM in June. It is clear that the overall daily production is higher in June than in January.

The evolution of power to water ratio exhibits similar behaviors for June and January characterized by a sharp decrease at morning followed by a constant value and increase at the end of the day.

5. Conclusion

A thermodynamic analysis of a poly-generation system powered by solar energy using parabolic trough solar collectors was developed. The system is composed of an organic Rankine cycle (ORC), a multiple effect distillation and an absorption cooling unit.

The performance of the poly-generation plant is investigated under Riyadh weather conditions and for several conditions of the operating parameters. Results on the performance of the poly-generation system were expressed using the energy and exergy efficiencies. Specifically, energy utilization factor, artificial thermal efficiency, fuel energy saving factor and exergy efficiency were introduced and used as plant performance indicators. Although, these indicators, except the exergy efficiency, conserve a trend similar to the direct normal irradiation intensity, their numerical values are dispersed and quite different in some cases. Moreover, they might lead to different conclusions. Thus, the assessment of the performance of poly-generation systems depends on the criterion used. The exergy efficiency and fuel energy saving factor give close values. The fresh water production rate and the power to water ratio were also evaluated for two representative days in June and January of 2013 in Riyadh.

It is important to mention finally that more accurate and adequate assessment requires the inclusion of other aspects such as cost, environmental impacts and sustainability.

Acknowledgment

The authors extend their appreciation to the Deanship of Scientific Research at King Saud University (Research group project No: RGP-VPP-091).

References

[1] Combined heating and power and emissions trading: options for policy makers, International Energy Agency, 2008, p. 27.
[2] I. Dincer, Renewable energy and sustainable development: a crucial review. Renew. Sustain. Energy Rev., 4(2) (2000) 157–175.
[3] P. Ahmadi, I. Dincer, Exergo-environmental analysis and optimization of a cogeneration plant system using Multimodal Genetic Algorithm (MGA) Energy, 35 (2010), 5161–5172.
[4] P. Ahmadi, M.A. Rosen, I. Dincer, Greenhouse gas emission and exergo-environmental analyses of a trigeneration energy system. Int. J. Greenhouse Gas Control, 5(6) (2011) 1540–1549.
[5] Z.H. Yao, Z.F. Wang, Z.W. Lu, X.D. Wei, Modeling and simulation of the pioneer 1MW solar thermal central receiver system in China, Renewable Energy, 34 (2009) 2437–2446.
[6] X. Li, W.Q. Kong, Z.F. Wang, C. Chang, F.W. Bai, Thermal model and thermodynamic performance of molten salt cavity receiver, Renewable Energy, 35 (2010) 981–988.

[7] W. Han, H.G. Jin, J.F. Su, R.M. Lin, Z.F. Wang, Design of the first Chinese 1MW solar-power tower demonstration plant, Int. J. Green Energy, 6 (2009) 414–425.
[8] P. Ahmadi, I. Dincer, Rosen M.A., Exergo-environmental analysis of a tri-generation system based on micro gas turbine and organic Rankine cycles. In: Proceedings of the global conference on global warming 2011, Lisbon, Portugal; 11–14 July 2011.
[9] L.M. Serra, M.A. Lozano, J. Ramos, A.V. Ensinas, S.A. Nebra, Poly-generation and efficient use of natural resources. Energy, 34 (2009) 575–586.
[10] J.D. Nixon, P.K. Dey, P.A. Davies. The feasibility of hybrid solar-biomass power plants in India, Energy, 46 (2012) 541–554.
[11] H. Zhai, Y.J. Dai, J.Y. Wu, R.Z. Wang. Energy and energy analyses on a novel hybrid solar heating, cooling and power generation system for remote areas. Appl. Energy, 86 (2009) 1395–1404.
[12] F.A. Al-Suleiman, I. Dincer, F. Hamdullahpur, Energy and exergy analyses of a biomass tri-generation system using an organic Rankine cycle, Energy, 45 (2012) 975–985.
[13] D. Maraver, J. Uche, J. Royo, Assessment of high temperature organic Rankine cycle engine for poly-generation with MED desalination: A preliminary approach, Energy Convers. Manage., 53 (2012) 108–117.
[14] Y. Wang, Y. Huang, E. Chiremba, A.P. Roskilly, N. Hewitt, Y. Ding, D. Wu, H. Yu, X. Chen, Y. Li, J. Huang, R. Wang, J. wu, Z. Xi, C. Tan, An investigation of a house hold size tri-generation running with hydrogen, Appl. Energy, 88 (2011) 2176–2182.
[15] C. Ugur, K. Comakli, F. Yuksel, The role of co-generation systems in sustainability of energy, Energy Convers. Manage., 63 (2012) 196–202.
[16] M. Kanoglu, I. Dincer, d M.A. Rosen, Understanding energy and exergy efficiencies for improved energy management in power plants, Energy Policy, 35 (2007) 3967–3978.
[17] I. Dincer, and M.A. Rosen, Exergy, Energy, Environment and Sustainable Development, Elsevier, 2nd ed., 2013, p. 537.
[18] I. Dincer, and H. Al-Muslim, Thermodynamic analysis of reheat cycle steam power plants. Int. J. Energy Res. 25 (2001) 727–739.
[19] E. Minciuc, O. Le Corre, V. Athanasovici, M. Tazerout, I. Bitir, Thermodynamic analysis of tri-generation with absorption chilling machine. Appl. Thermal Eng., 23 (2003) 1391–1405.
[20] P. Ahmadi, I. Dincer, M.A. Rosen. Exergo-environmental analysis of an integrated organic Rankine cycle for trigeneration, Energy Convers. Manage., (2012) 447–453.
[21] M. Ameri, A. Behbahaninia, A. Abbas Tanha, Thermodynamic analysis of a tri-generation system based on micro-gas turbine with a steam ejector refrigeration system Energy, 35(5) (2010) 2203–2209.
[22] H. Li, L. Fu, K. Geng, Y. Jiang, Energy utilization evaluation of CCHP systems, Energy Buildings, 38(3) (2006) 253–257.
[23] E. Cardona, and A. Piacentino, A methodology for sizing a tri-generation plant in Mediterranean areas, Appl. Thermal Eng., 23(13) (2003) 1665–1680.
[24] A.M. E1-Nashar, Cogeneration for power and desalination - State of the art review, Desalination, 134 (2001) 7–28.
[25] A.M. Helal, Hybridization - a new trend in desalination, Desal. Wat. Treat., 3 (2009) 120–135.
[26] G.M. Zak, A. Ghobeity, M.H. Sharqawy, A. Mitsos, A review of hybrid desalination systems for co-production of power and water: analyses, methods, and considerations, Desal. Wat. Treat., 51 (2013) 5381–5401.
[27] P. Palenzuela, G. Zaragoza, D.C. Alarcón-Padilla, J. Blanco, Evaluation of cooling technologies of concentrated solarpower plants and their combination with desalination in the Mediterranean area, Appl. Thermal Eng., 50(2) (2013) 1514–1521.
[28] Y. Zhao, A. Akbarzadeh, J. Andrews, Simultaneous desalination and power generation using solar energy, Renewable Energy, 34(2) (2009) 401–408.
[29] P. Palenzuela, G. Zaragoza, D.C. Alarcón-Padilla, E. Guillén, M. Ibarra, J. Blanco, Assessment of different configurations for combined parabolic-trough (PT) solar power and desalination plants in arid regions, Energy, 36(8) (2011) 4950–4958.
[30] B.F. Tchanche, G. Papadakis, G. Lambrinos, A. Frangoudakis, Fluid selection for a low-temperature solar organic Rankine cycle, Appl. Thermal Eng., 29 (2009) 2468–2476.
[31] G. Pei, L. Jing, J. Ji, Analysis of low temperature solar thermal electric generation using regenerative organic Rankine cycle, Appl. Therm. Eng., 30 (2010) 998–1004.
[32] www.Skyfuel.com "Sky Trough @Fact sheet 2011".
[33] Therminol. Heat transfer fluids by Solutia Inc., Therminol VP-1. www.therminol.com/pages/products/vp-1.asp; Aug. 2012.
[34] M.J. Montes, A. Abanades, J.M. Martinez-Val, Performance of a direct steam generation solar thermal power plant for electricity production as a function of the solar multiple. Sol Energy, 83 (2009) 679–689.
[35] S. Kalogirou, Solar energy engineering: processes and systems, Elsevier, (2009) p. 760.
[36] S.A. Klein, Engineering equation solver (EES), Academic commercial Version 9.725, F-chart; 2014. http://www.fchart.com/ees/.
[37] S. Kalogirou, Solar thermal collectors and applications, Progr. Energy Combust. Sci., 30 (2004) 231–295.
[38] J. Duffie, W. Beckman, Solar engineering of thermal processes, John Wiley & Sons, Inc., Fourth edition (2013) p. 910.
[39] H. El-Dessouky, I. Alatiqi, S. Bingulac, H. Ettouney, Steady-state analysis of the multiple effect evaporation desalination process, Chem. Eng. Technol., (1998) 437–451.
[40] K.H. Mistry, M.A. Antar, J.H. Lienhard V, An improved model for the multiple effect distillation, Desal.Wat. Treat., 51 (2013) 807–821.
[41] R.K. Kamali, A. Abbassi, S.A. Sadough Vanini, M. Saffar Avval, Thermodynamic design and parametric study of MED-TVC, Desalination, 222 (2008) 596–604.
[42] D. Zhao, J. Xue, Shi Li, H. Sun, Q. Zhang, Theoretical analyses of thermal and economical aspects of multi-effect distillation desalination dealing with high-salinity wastewater, Desalination, 273 (2011) 292–298.
[43] Y.A. Cengel, M.A.Boles, Thermodynamics: An engineering Approach, 6th ed., Mc Graw Hill, (2007), p. 976.
[44] A. Bejan, G. Tsatsaronis, M. Moran, Thermal design and optimization, John Wiley and Sons, (1996) p. 542.
[45] C. Kutscher, F. Burkholder, K. Stynes, Generation of Parabolic Trough Collector Efficiency curve from Separate measurements of outdoor optical efficiency and indoor receiver heat loss, National Renewable Energy Laboratory Presented at Solar PACES 2010 Perpignan, France, p. 7.
[46] H.D. Madhawa-Hettiarachchi, M. Golubovic, W.M. Worek, Y. Ikegami, Optimum design criteria for an Organic Rankine cycle using low-temperature geothermal heat sources. Energy, 32(9) (2007) 1698–1706.
[47] M. Balghouthi, M.H. Chahbani, A. Guizani. Feasibility of solar absorption air conditioning in Tunisia. Building Environ., 43 (2008) 1459–1470.